

X-ray diffraction studies of oriented lipid bilayers

J. Katsaras

Abstract: This brief review of the X-ray diffraction technique used to study oriented lipid bilayer systems is primarily intended to demonstrate to the nonspecialist in the lipid field the amount of detailed information that can be obtained simply by visually inspecting the diffraction pattern and making some measurements with a ruler and protractor. The information that can be extracted from X-ray diffraction data is illustrated by selected examples of our most recent work.

Key words: X-ray diffraction, oriented multibilayers, electron density profiles, subgel phase, phase problem.

Résumé : Le but principal de cette brève revue de la technique de diffraction des rayons X utilisée pour étudier les systèmes de bicouches lipidiques orientées est de démontrer, aux personnes non spécialisées dans le domaine des lipides, la quantité d'informations détaillées pouvant être obtenues simplement en regardant le spectre de diffraction et en effectuant certaines mesures avec une règle et un rapporteur. Certains exemples tirés de notre plus récent travail illustrent l'information pouvant être obtenue des résultats de diffraction des rayons X.

Mots clés : diffraction des rayons X, bicouches orientées, spectres de densité électronique, phase presque gel, problème de phase.

[Traduit par la rédaction]

Introduction

Lipids are of fundamental importance as they are the main constituents of biological membranes. They are amphiphilic and, when hydrated, self-assemble into a variety of structural phases (Tardieu et al. 1973). Since the proposal of the fluid mosaic model of membrane structure by Singer and Nicolson (1972), much effort has been expended in understanding the structure of model membrane systems and their relevance to biological membranes. Studying the structural polymorphism observed in many simple lipid-water systems allows us to gain an understanding of the intermolecular forces that can exist in a biological membrane and that can affect the organization and function of proteins (Gruner 1992). Most recently, an understanding of the structural polymorphism and stability of pure lipid vesicles is proving to be essential in the development of liposome-mediated drug delivery systems (Bentz et al. 1992).

Received January 12, 1995. Accepted June 6, 1995.

Abbreviations: 1D, one dimensional; PSD, position-sensitive detector; 2D, two dimensional; FWHM, full width at half-maximum; DPPC, 1,2-dipalmitoyl-*sn*-glycero-3-phosphatidylcholine; L_{β} , gel phase; RH, relative humidity; 3D, three dimensional; DSC, differential scanning calorimetry; T_c , temperature of crystallization; POPE, 1-palmitoyl-2-oleoyl phosphatidylethanolamine.

J. Katsaras. Atomic Energy of Canada Limited, Chalk River Laboratories, Chalk River, ON K0J 1J0, Canada.

In recent years, there has been a great deal of interest in determining the precise nature of lipid phases and phase transitions. As such, X-ray diffraction has proven to be one of the most powerful and direct methods for characterizing lipid-water systems (e.g., Smith et al. 1988; Hentschel and Rustichelli 1991; Katsaras et al. 1992a; 1992b; Weiner and White 1992; Katsaras et al. 1993; Tristram-Nagle et al. 1993; McIntosh and Simon 1993). One of the most comprehensive studies on the structure and polymorphism of lipid-water systems using X-ray diffraction was performed by Tardieu et al. (1973). They clearly demonstrated, using powder samples, the varied characteristics of lipids and their ability to form a variety of phases.

In this article we describe, for the nonspecialist in the field, the information that one can obtain using oriented lipid bilayer systems and the diffraction method. We illustrate the information by using selected examples of our most recent work. Although we specifically refer to X-ray diffraction data, complementary experiments using neutrons instead of X-rays can be carried out in a similar fashion. For comprehensive reviews of X-ray diffraction and bilayers we refer the reader to articles by Levine (1973), Mitsui (1978), Franks and Lieb (1981), and Blaurock (1982).

Instrumentation for X-ray studies

X-ray sources

Most X-ray diffraction studies of model membrane systems

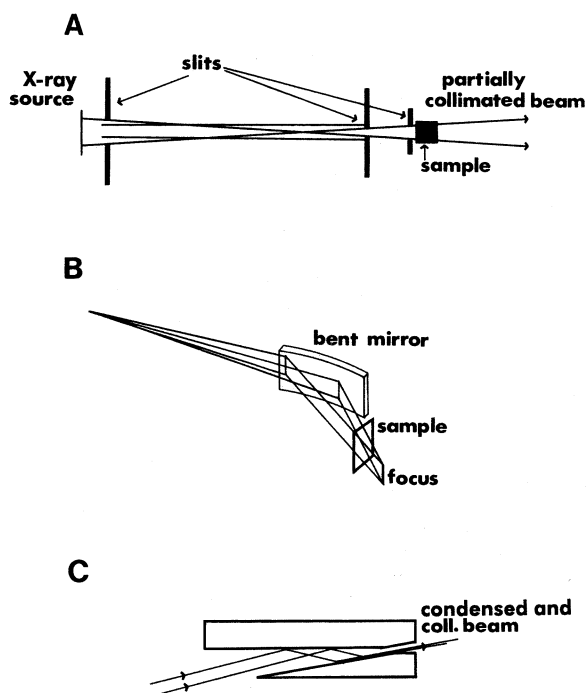
use X-rays produced by sealed-tube or rotating anode X-ray sources. These sources are today termed conventional and generally produce beams that are 10–100 times less intense than X-ray beams derived from synchrotron sources (Phillips 1985). Even though conventional sources offer less intensity compared with synchrotrons, they make up for this shortcoming by being reliable, inexpensive, and easily accessible. However, sometimes the high brilliance and tunability (choice of a variety of wavelengths) of a synchrotron source may be necessary for a particular experiment and can more than outweigh the inconvenience of a distant facility and limited access time. For contributions to dynamic structural changes of muscle made possible by high-brilliance synchrotron radiation sources, the reader is referred to a detailed article by Wakabayashi and Amemiya (1991).

X-rays are principally produced from two effects: (i) drastic deceleration of fast-moving electrically charged particles (conventionally, this effect occurs when fast-moving electrons strike a solid target material, e.g., copper); (ii) ejection of an orbital electron by some means, allowing an electron from a higher orbital to “drop” into the vacant orbital and in so doing emitting electromagnetic radiation. The characteristic X-ray spectrum as derived from conventional sources is a superposition of the above-mentioned two effects (Cullity 1978). Since only a fraction of the kinetic energy of the electrons is converted into the production of X-rays, the target material is water-cooled to prevent its melting. The rate of heat removal from the anode determines the maximum power load. As a result of their design, rotating anodes can sustain power loadings of 7–45 times more than sealed tubes, resulting in beams of high brilliance (Phillips 1985). Therefore, the bombardment of the copper target by high-speed electrons, along with the use of a nickel filter (Cullity 1978), results in X-rays with a wavelength of $\approx 1.54 \text{ \AA}$ ($1 \text{ \AA} = 0.1 \text{ nm}$). On the other hand, radiation from synchrotron radiation X-ray sources is obtained from storage rings that contain charged particles undergoing a curved motion at relativistic velocities. Further details describing the various aspects of rotating anode and sealed-tube sources can be found in an article by Phillips (1985).

Optical arrangements

In Figs. 1A and 1B, we present two of the most common optical arrangements used in X-ray diffraction studies of model membranes. The pinhole camera illustrated in Fig. 1A represents the simplest optical arrangement. The X-ray beam is defined by two slits, and a third slit, just before the sample, is used to limit the angular divergence and to reduce parasitic scatter from the defining slits. The major drawback of this optical arrangement is that to get good angular resolution, intensity is sacrificed. To overcome the problems of the pinhole camera, many experimental configurations use either single- (Fig. 1B) or double-focusing mirror assemblies to obtain line- or point-focused beams, respectively (Phillips and Rayment 1985). These systems use the total external reflection of the mirrors to “focus” the X-ray beam onto the detector, resulting in intense X-ray beams of small angular divergence. Assuming that sample size is not a limiting factor and that one is only interested in recording 1D data, then the single-mirror arrangement is preferable to the double mirror arrangement, because for example, a rotating anode can handle a much greater power load in the line-focus mode than in the point-

Fig. 1. Commonly used optical arrangements in X-ray diffraction experiments of model membranes. (A) Pinhole collimation. (B) Focusing bent glass mirror. Using a single bent mirror results in a line beam, while using two perpendicularly bent mirrors results in a point beam. Bending the mirrors focuses the X-ray beam. (C) Double-reflection condensing-collimating channel-cut monochromator used on both synchrotron and conventional sources. Silicon or germanium crystals are usually the material of choice. Coll., collimated.



focus mode and can result in data acquisition times being shorter. However, point-focused beams are used exclusively when high order-to-order resolution in two dimensions is required. The above mentioned optical arrangements can be easily constructed by a competent machine shop. Instead of two mirrors, one can use a mirror-monochromator arrangement, depending on the desired angular resolution and geometrical parameters and characteristics of the diffractometer (Wakabayashi and Amemiya 1991). It should be noted, that mirror assemblies, unlike crystal monochromators, cannot resolve the K_{α_1} and K_{α_2} lines.

Most recently, there has been great interest in the development of condensing-collimating channel-cut monochromators (Fig. 1C), which produce highly collimated X-ray beams of substantial intensity suitable for both synchrotron and conventional sources (Wilkins and Stevenson 1988). Such monochromators can prove very useful for high-resolution small-angle X-ray scattering experiments, since they can provide tailless beams of small cross section. For a review of X-ray monochromators used at different synchrotron facilities, the reader is referred to an article by Caciuffo et al. (1987), while a good hands-on approach to the double-focusing mirrors is given by Phillips and Rayment (1985).

Detectors

The oldest form of X-ray detector is photographic film, consisting of a light-sensitive layer of material (silver halide)

deposited onto a transparent base (gelatin). The advantages of film over other types of detectors are the following: (i) it has a spatial resolution of about of 1 μm ; (ii) it is inexpensive and provides a visual record without the use of electronics; and (iii) film can be curved to the correct radius of curvature and has a uniform response over its entire area. Film does, however, have certain disadvantages such as the following: (i) intrinsic chemical fogging that degrades the signal to noise ratio; (ii) low absorption efficiency; (iii) limited dynamic range; and (iv) unsuitability for time-resolved experiments (Amemiya et al. 1988). Taking everything into consideration, film does not compare favourably with the other detectors that will be discussed here.

One type of detector that can provide fast data acquisition and a very good signal to noise ratio is the PSD. The detector is basically a gas proportional chamber containing an anode housed in a sealed pressurized cell (≈ 12 bar, 1 bar = 100 kPa). The positional information along the anode wire is determined, using a delay line, via the difference in time between the pulses propagated towards each end of the wire. 1D detectors of this type are commonly used and are relatively inexpensive to set up. However, multiwire area proportional counters used for structural determination of relatively large biological molecules are expensive and have a small active area necessitated by the high pressure of the filling gas (Ar-CH₃ or Xe-CH₃). On the other hand, with appropriate electronics, 1D and 2D PSDs are ideally suited to time-resolved studies.

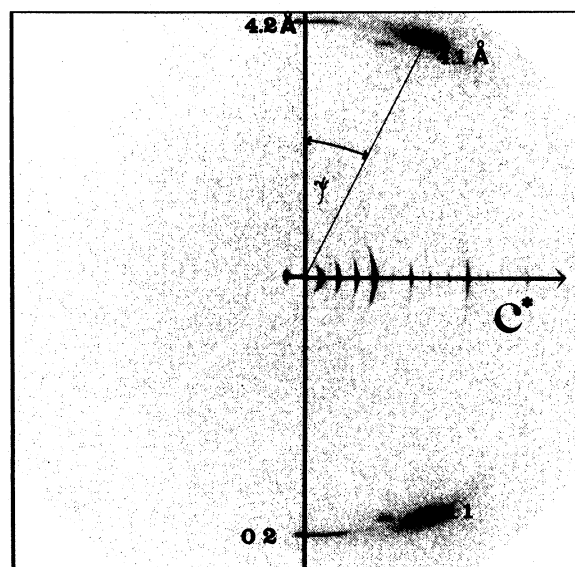
Most recently, a new type of X-ray detector called an imaging plate has been developed and essentially eliminates the limitations of photographic film and PSDs (Amemiya et al. 1988; Amemiya and Wakabayashi 1991). The system is based on a thin flexible plastic plate coated with a photostimulable phosphor (BaFBr:Eu²⁺) capable of temporarily storing a 2D X-ray image in the form of quasistable colour centres. The image is subsequently read out using a laser and by digitally recording the photostimulated luminescence, which is proportional to the absorbed X-ray intensity. The image plate can then be reused by irradiating it with visible light. The articles by Amemiya et al. (1988) and Amemiya and Wakabayashi (1991) give a good description of the principle and performance of the imaging plate detector and its application to X-ray diffraction of muscle. At present, the major drawback of the imaging plate detector is its cost.

The data presented in this paper were collected using an 18-kW Rigaku Rotaflex RU300 rotating anode generator and a 2D Marresearch imaging-plate detector having a plate diameter of 180 mm and a pixel size of 150 \times 150 μm . Monochromatization of the Cu radiation was achieved using a flat graphite crystal having a mosaic spread of $0.4 \pm 0.1^\circ$ FWHM₀₀₂. The spot size, as defined by three sets of vertical and horizontal slits (similar to Fig. 1A), was approximately 0.5 \times 0.5 mm and the sample to film distance was 185 ± 1 mm.

Sample preparation

Typical lipid-water samples used in X-ray diffraction studies can either be oriented onto a curved glass substrate (e.g., Torbet and Wilkins 1976; Katsaras et al. 1993) or unoriented, whereby a lipid-water dispersion is deposited into a thin-wall (10 μm) glass or quartz capillary tube (diameter = 1–2 mm) and flame sealed (e.g., Franks and Lieb 1981). Oriented mul-

tilayers are easily obtained by depositing a lipid-organic solvent solution on a substrate and allowing the organic solvent to slowly evaporate. For the most part, more information can be obtained by using oriented multibilayer samples than from a random dispersion of stacked membranes (Franks and Lieb 1981). However, sometimes conditions dictate the use of unoriented samples (e.g., excess water). In this paper all of the data presented were obtained using oriented multibilayer stacks.



tilayers are easily obtained by depositing a lipid-organic solvent solution on a substrate and allowing the organic solvent to slowly evaporate. For the most part, more information can be obtained by using oriented multibilayer samples than from a random dispersion of stacked membranes (Franks and Lieb 1981). However, sometimes conditions dictate the use of unoriented samples (e.g., excess water). In this paper all of the data presented were obtained using oriented multibilayer stacks.

Structural studies of lipid multibilayers

To reconstruct the structure of a molecule, one must accurately determine the various structure factors ($F_h = |F_h|e^{i\phi_h}$). Since the structure factor F_h is a complex number of magnitude $|F_h|$ and phase term $e^{i\phi_h}$, it is not possible to experimentally measure F_h directly. This presents us with the infamous phase problem. However, a surprisingly large amount of information can be obtained by simply determining the positions and analyzing the shapes of the diffraction maxima from an X-ray diffraction pattern.

Detailed structural information without intensity measurements:

Figure 2 shows a diffraction pattern obtained using oriented DPPC bilayers in the gel $L_{\beta'}$ or more precisely, the L_{β_1} phase (Smith et al. 1988). The $L_{\beta'}$ phase is in fact three distinct 2D phases that are distinguishable by their hydrocarbon chain tilt direction. In the low-RH $L_{\beta'}$ and high-RH L_{β_1} phases, the hydrocarbon chains are tilted between nearest neighbours and toward nearest neighbours, respectively, while the L_{β_1} is an intermediate phase (Smith et al. 1988). It should be noted that as a result of our diffraction geometry, only half of the diffrac-

tion pattern is recorded (Katsaras et al. 1992*b*, 1993). From the reflections along the c^* axis, the bilayer repeat distance d can easily be determined using Bragg's law; $h\lambda = 2d \sin \theta_B$, where θ_B is the Bragg angle, h is the order number, and λ is the wavelength of the X-ray radiation. The scattering angle θ_S is simply equal to $2\theta_B$. Also, the most commonly used wavelength for lipid bilayer studies is 1.54 Å, obtained using a Cu target. Besides obtaining the bilayer repeat distance, the organization of the hydrocarbon chains in the plane of the bilayer can be determined from the wide-angle reflections that have been labelled (1 1) and (0 2) in Fig. 2. In the plane of the bilayer, the hydrocarbon chains are packed in such a fashion that they are surrounded by six neighbors. If the hydrocarbon chains of the lipid molecules were not tilted with respect to the bilayer normal (termed the L_B phase), then only two wide-angle reflections centered on the equatorial axis (the axis that is perpendicular to the c^* axis) would be observed (Katsaras et al. 1993) and would indicate hexagonal symmetry. In Fig. 2 this is not the case. The wide-angle reflections can be explained in terms of a centered rectangular lattice (in which the hexagon is slightly distorted from regularity) with the DPPC molecules tilted towards their nearest neighbors (Leadbetter et al. 1979; Smith et al. 1988). The tilt angle θ , to a first approximation, can then be calculated relatively easily using $\sin \psi = \cos 30^\circ \sin \theta$, where ψ is the angle made with the equatorial axis by the 4.1-Å wide-angle reflection and is measured directly from the diffraction pattern (Levine 1973; Hentschel et al. 1980). If the hydrocarbon chains were tilted in a direction between nearest neighbors, referred to as the L_{Bf} phase, then each quadrant of the diffraction pattern would contain two off-equatorial reflections and θ would simply be equal to the angle made by the (2 0) reflection (Leadbetter et al. 1979; Smith et al. 1988; Katsaras et al. 1992*b*). In addition, the fact that the lengths (direction parallel to c^*) of the hydrocarbon chain reflections are approximately equal to the separation between successive lamellar reflections indicates that the L_{Bf} phase is not a 3D structure but rather is composed of 2D structures with no out-of-plane correlations (Smith et al. 1988). Therefore, by simply taking a 2D X-ray diffraction pattern of an oriented lipid system and doing some very simple measurements, we were able to determine the following: (i) the hydrocarbon chain tilt angle θ ; (ii) the direction of tilt with respect to the quasi-hexagonal hydrocarbon chain lattice; (iii) the bilayer repeat spacing d ; and (iv) the fact that these systems are not 3D crystals but rather 2D structures.

Structure of DPPC subgel phase bilayers

In 1980, Chen et al. (1980) observed a new phase transition, centered at about 18°C, in a DPPC multilamellar suspension using DSC. Until then, DPPC suspensions were known to have only two thermotropic phase transitions: the main gel-to-liquid crystalline phase transition ($T_c \approx 41^\circ\text{C}$) and a broader so-called pretransition ($T_c \approx 35^\circ\text{C}$). However, this newly discovered phase, referred to as the subgel, was observed only after Chen et al. stored the multilamellar suspension of DPPC at $\approx 0^\circ\text{C}$ for several days (Chen et al. 1980). Since then, there have been many diffraction experiments carried out to characterize the structure of this phase (e.g., Fuldner 1981; Ruocco and Shipley 1982; Stümpel et al. 1983; McIntosh and Simon 1993; Tristram-Nagle et al. 1994). Despite these studies, the structure of subgel DPPC multilayers had remained elusive until recently.

Fig. 3. 2D diffraction pattern of oriented DPPC subgel phase bilayers. The reflections at $1/10.0$ and $1/6.8 \text{ \AA}^{-1}$ arising from the 2D molecular lattice have been labelled (0 1) and [(1 $\bar{1}$), (1 1)], respectively. These reflections, as a result of the ordering of the DPPC molecules, are split up into discrete equidistant spots whose separation corresponds to $\approx 40 \text{ \AA}$, which is typically the distance between the phosphoryl groups across the bilayer. Therefore, the modulation in intensity of the (0 1) and [(1 $\bar{1}$), (1 1)] reflections indicate the presence of correlations in the head-group ordering across the bilayer. The tilt angle θ for this system was calculated to be $34.5 \pm 1.0^\circ$ (Katsaras et al. 1995).

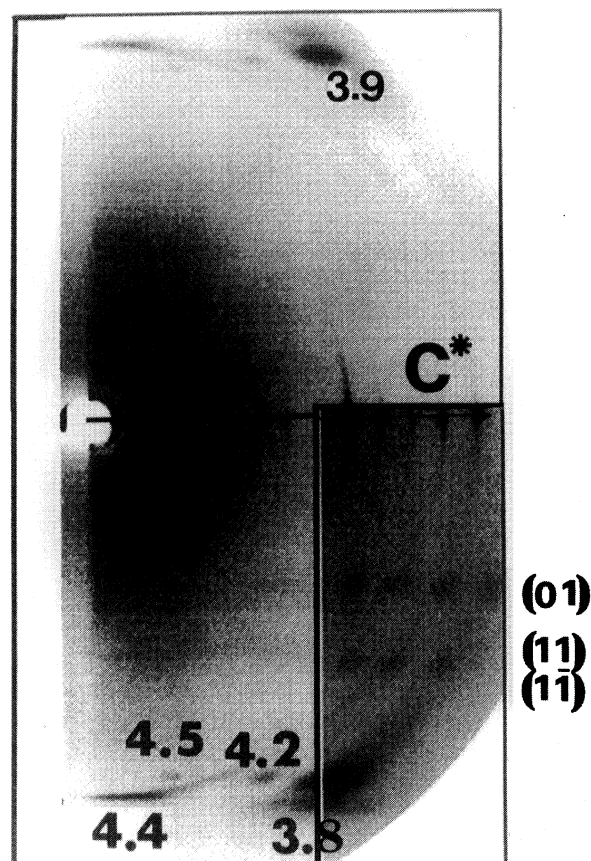


Figure 3 shows the diffraction pattern from subgel phase DPPC bilayers. Visual inspection of the diffraction patterns in Figs. 2 and 3 shows that the main differences between the two phases of DPPC lie with the hydrocarbon chain reflections and the two additional reflections at $1/6.8$ [(1 1), (1 $\bar{1}$)] and $1/10.0$ (0 1) \AA^{-1} present in subgel phase DPPC bilayers (Fig. 3). The fact that the (1 1) hydrocarbon chain reflection in the L_{Bf} phase (Fig. 2) splits into two in the subgel phase (Fig. 3) implies that the hydrocarbon chain lattice in the subgel phase is no longer rectangular but oblique ($\gamma \neq 90^\circ$). The reflections corresponding to repeat spacings of 4.2 and 4.5 Å lie in a straight line along with the 3.9 Å reflection and are due to the form factor of the finite length hydrocarbon chains (Smith et al. 1990). As a result, they do not correspond to any lattice spacings. However, the reflections at $1/6.8$ and $1/10.0 \text{ \AA}^{-1}$ are of greater interest.

The gel-to-subgel phase transition can be regarded as a disorder-order transition in which the subgel phase ends up pos-

Fig. 4. The possible molecular arrangements in the superlattice obtained by connecting the hydrocarbon chains in various ways. ●, hydrocarbon chains; ■ phosphorylcholine headgroups. The molecular lattice is represented by a series of broken lines and has dimensions $a = 9.4 \text{ \AA}$, $b = 10.0 \text{ \AA}$, and $\gamma = 90^\circ$. By connecting the two nearest neighbor hydrocarbon chains with one headgroup we obtain a lipid molecule. The molecular lattice, which contains two lipid molecules, was constructed from a hydrocarbon sublattice of dimensions $a = 5.3$, $b = 8.8$, and $\gamma = 94^\circ$. The molecular arrangements shown in Figs. 4A–4C belong to the plane group $p2$, while the rest (Figs. 4D–4F) belong to $p1$.

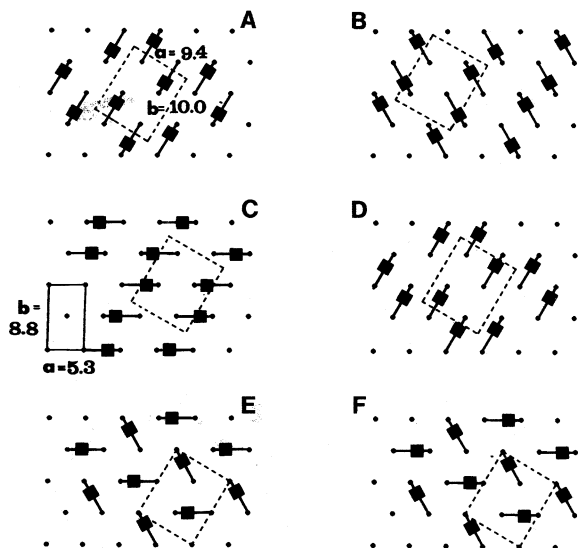


Table 1. Calculated repeat spacings for the various $(h\ k)$ reflections of the molecular superlattice (shown in Fig. 4).

$(h\ k)$	$d(\text{\AA})$
0 1	10.0
1 0	9.4
1 1	6.8
1 $\bar{1}$	6.8
0 2	5.0
$\bar{1}$ 2	4.4
2 0	3.9*
1 2	3.8*

The projections of the (2 0) and (1 2) reflections onto the equatorial axis (perpendicular to c^) correspond to lattice spacings of 4.7 and 4.4 \AA , respectively. Their repeat spacings, as a result of the hydrocarbon chain tilt, do not correspond to lattice dimensions.

sessing a molecular lattice. In the gel phase (Fig. 2), the hydrocarbon chains of the DPPC molecules form a centered rectangular lattice ($a = 5.5 \text{ \AA}$ and $b = 8.5 \text{ \AA}$), while the phosphorylcholine headgroups rotate freely. Since the DPPC molecules in the plane of the bilayer are not ordered, we can then characterize the gel phase as being disordered. In the subgel phase (Fig. 3), the hydrocarbon chain reflections are not much

different than those in the gel phase and form a lattice of dimensions $a = 5.3 \text{ \AA}$ and $b = 8.8 \text{ \AA}$. Therefore, the additional reflections at $1/6.8$ and $1/10.0 \text{ \AA}^{-1}$ arise from the ordering of the DPPC molecules themselves and the formation of a 2D molecular lattice (Katsaras et al. 1995), effectively freezing out the headgroup motions (Katsaras 1995). This is a classic disorder–order transition. There is little alteration to the parent lattice formed by the hydrocarbon chains and the extra lines that appear are due to the 2D molecular lattice or superlattice (Cullity 1978). Since each DPPC molecule consists of two hydrocarbon chains linked by a glycerol backbone carrying the headgroup, it is possible to construct many molecular lattices from a given hydrocarbon sublattice. Interestingly, there is a unique molecular lattice, shown in Fig. 4, whose repeat spacings due to the various lattice planes (Table 1) are in excellent agreement with the experimental data in the literature (Table 2). Also, the determination of the lattice parameters of the molecular lattice do not by themselves lead to an understanding of the arrangement of the lipid molecules in the unit cell (Katsaras et al. 1995). However, in the present case, the existence of two commensurate lattices restricts the number of possible molecular arrangements in the bilayer to six (Fig. 4). Finally, the reflections at $1/6.8$ and $1/10.0 \text{ \AA}^{-1}$ appear in the form of long bars parallel to the c^* axis (Fig. 3) and are consistent with their origin in the ordering of relatively short entities, like the headgroups, in the plane of the bilayer. The period of modulation of the intensity along these reflections is approximately 40 \AA and corresponds to the separation of the headgroups across the bilayer (Katsaras et al. 1995). This repeat spacing is a measure of the thickness of a single bilayer and is in good agreement with the value obtained from 1D electron density profiles of subgel phase DPPC multibilayers constructed to a resolution of $\approx 4 \text{ \AA}$ (Katsaras 1995).

From the examples presented in the Detailed structural information without intensity measurements and the Structure of DPPC subgel phase bilayer sections, the reader should be able to deduce that there are few techniques, if any, that yield so much detailed structural information from such simple measurements. The geometrical relationships for the example in Detailed structural information without intensity measurements section have been worked by various groups (e.g. Levine 1973; Hentschel et al. 1980; Hentschel and Rustichelli 1991) and the reader only needs to apply them. The results obtained for the example presented in the structure of DPPC subgel phase bilayer section may not be obvious to the reader with no background in fiber diffraction but are presented to further demonstrate the detail made available by this technique.

Solving of the phase problem and reconstruction of the electron density profiles

In the preceding section we attempted to demonstrate to the reader that a great deal of structural information about a bilayer system can be obtained by performing some simple positional measurements. However, even more structural information can be obtained if we can solve the phase problem.

As mentioned in an earlier section, the structure factor F_h has a magnitude of $|F_h|$ and a phase term $e^{i\phi_h}$. Although $|F_h|$ is a measurable quantity, the phase angle ϕ_h is not and can assume any value from 0 to 2π , with only one phase angle being correct for a given $|F_h|$. However, if the structure being studied is

Table 2. Experimentally observed repeat spacings from subgel DPPC multilayers.*

Füldner 1981	McIntosh and Simon 1993	Ruocco and Shipley 1982	Stümpel et al. 1983	Tris-Nagle et al. 1994	Katsaras et al. 1995 [†]	Katsaras et al. 1995 [‡]
10.0	9.8	10.0	10.0	10.14	10.0 [§]	10.0 [§]
—	—	9.30	—	9.36	9.4 [§]	—
6.75	6.8	6.81	6.78	6.84	6.8 [§]	6.8 [§]
—	—	4.9	—	—	5.0 [§]	—
—	—	4.52	—	—	4.5	4.5
4.4	4.4	4.43	4.40	4.46	4.4	4.4
—	—	4.2	4.20	4.25	4.2	4.2
3.85	3.9	3.83	3.88	3.92	3.8–3.9	3.9
						3.8

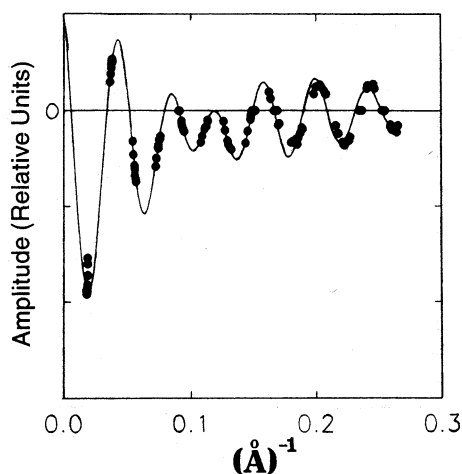
*These reflections are in addition to the lamellar reflections. All values are in Å; —, reflections not observed.

[†]Data obtained from excess water liposomes.

[‡]Data obtained from oriented samples.

[§]Reflections due to the ordering of the DPPC molecules.

Fig. 5. Structure factors (●) obtained in a series of swelling experiments at 20°C of partially dehydrated L_{β} POPE bilayers with a superimposed continuous Fourier transform (—) calculated for the 70% RH sample.



centrosymmetric, then the Fourier transform of a centrosymmetric function is real. This means that the structure factor F_h is given by either $+|F_h|$ or $-|F_h|$. As can be appreciated, this simplification of the structure factors greatly reduces the complexity of the phase problem. Finally, $|F_h| = \pm\sqrt{I_h}$, where I_h is the intensity of a Bragg reflection.

With lipid bilayers and biological centrosymmetric systems (e.g., nerve myelin sheath, visual cell outer segments), it is possible to assign phases by increasing the thickness of the water layer between the bilayers and mapping out the changes in intensity for the various Bragg reflections (Torbet and Wilkins 1976). This can be achieved by equilibrating the sample at different relative humidities using a variety of salt solutions. Once all the intensity data are obtained, the continuous Fourier transform can be reconstructed using the communication theory of Shannon (Shannon 1949; Sayre 1952). The continuous transform F_R is constructed by laying down the function $F_h(\sin \pi dx)/\pi dx$ at points $x = h/d$ ($h = 0, 1, 2, 3, \dots, n$) and adding. The sign of the amplitude is determined by the phase.

In Fig. 5, we present data from a series of X-ray swelling experiments for oriented multibilayers of POPE (Katsaras et al. 1993). As we swelled the bilayers, a different d is obtained, effectively sampling the Fourier transform F_R at different points $x = h/d$. If enough swelling states can be achieved, then the transform can be mapped out and the structure factors deduced. In addition, the experimental structure factors can be fitted by a single calculated continuous Fourier transform, which implies that the bilayer structure remains unchanged as a function of changes in hydration (Torbet and Wilkins 1976). The zero-order amplitude, necessary for the reconstruction of the continuous transform but whose accuracy is not crucial, is calculated by subtracting the electron density of water from the average electron density and multiplying by d (Katsaras et al. 1991).

As soon as the structure factors are obtained, the 1D electron density profile can be reconstructed using the formula

$$\rho(x) = \sum_{h=1}^{h_{\max}} |F_h| \cos(2\pi hx - \phi_h),$$

where $\rho(x)$ is the electron density function. The electron density profiles of POPE bilayers at three different RH values calculated from structure factors shown in Fig. 5 are presented in Fig. 6. Notice that the electron density profiles differ mainly in the separation of the phosphorylcholine headgroups. This makes physical sense, since the amount of water is being increased and the bilayers do not undergo any phase transitions; the expected change would be an enlarged water region (Katsaras et al. 1993). Figure 7 shows an electron density profile containing 1.5 bilayer units constructed to a resolution of ≈ 4 Å and a corresponding model of a lipid bilayer having its hydrocarbon chains tilted at an angle θ with respect to the bilayer normal (Katsaras 1995). The interpretation of 1D electron density profiles is by now well understood (e.g., Torbet and Wilkins 1976). The low electron density trough is attributed to the terminal methyl groups, while the maxima correspond to the phosphate moieties of the polar phosphorylcholine headgroups (highest electron density) and the ester groups of the hydrocarbon chains. The methylene groups of the hydrocarbon chains are depicted in the 1D profile as regions of relatively uniform electron density, while the region

Fig. 6. 1D electron density profiles of L_{β} POPE bilayers. (a) 0% RH ($d = 52.8 \text{ \AA}$); (b) 70% RH ($d = 54.1 \text{ \AA}$); and (c) 100% RH ($d = 55.5 \text{ \AA}$). Notice that the changes in d are attributable to the changes in the water region (region between adjacent bilayers) (Katsaras et al. 1993).

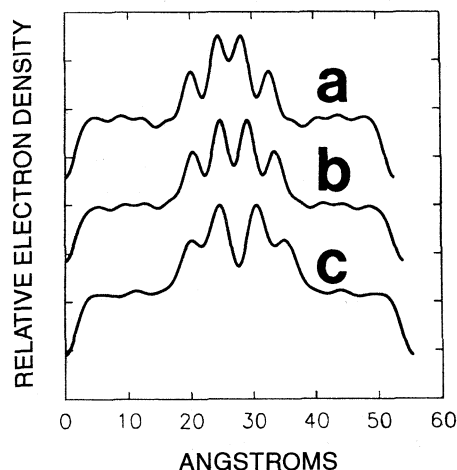
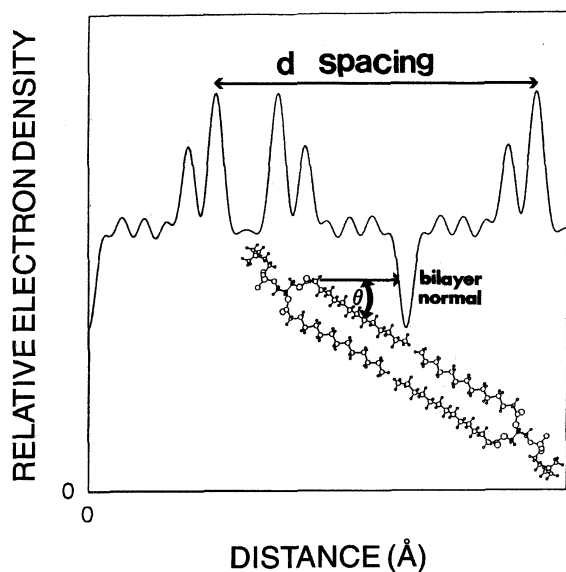


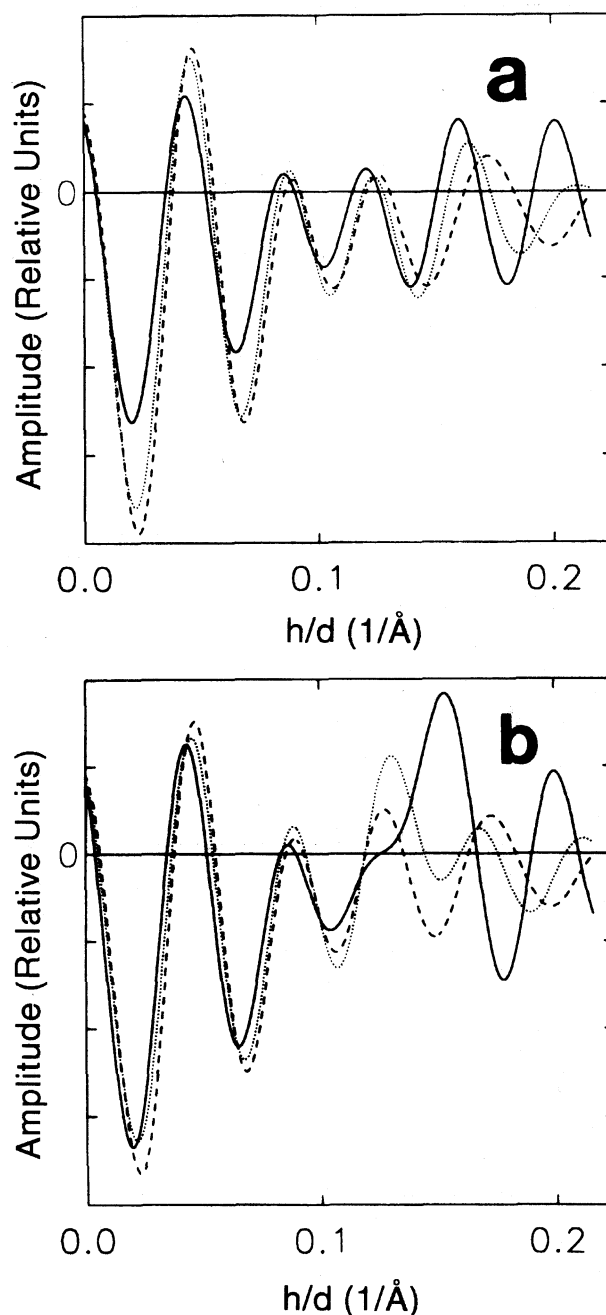
Fig. 7. 1D electron density profile showing 1.5 bilayer units constructed to a resolution of $\approx 4 \text{ \AA}$ and a corresponding lipid bilayer whose hydrocarbon chains are tilted at an angle θ with respect to the bilayer normal (Katsaras 1995).



between the two most electron dense peaks is generally known as the water region. The thickness of the water region gives some indication as to the relative amounts of water present in the sample.

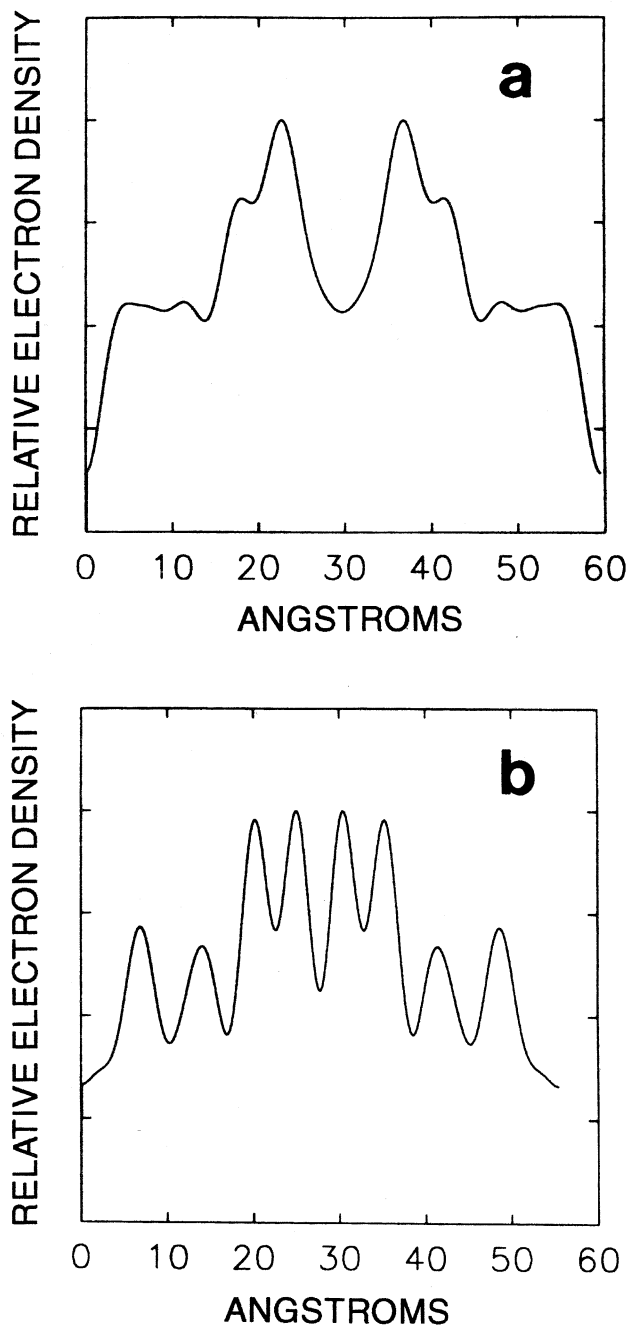
The hydrocarbon chains of POPE bilayers are not tilted ($\theta = 0^\circ$) and they remain unaffected with changes in hydration. However, this is not the case with some bilayer systems. For example, the tilt angle θ of DPPC bilayers increases with increasing levels of hydration up to a maximum of approximately 32° (Tardieu et al. 1973; Katsaras et al. 1992b). Therefore, this change in θ as a function of hydration complicates the solution of the phase problem. In this case, where changes in hydration result in changes to the bilayer (motif), the correct

Fig. 8. (a) Continuous Fourier transforms of L_{β} DPPC bilayers at RH values of 0% (---), 75% (···), and 90% (—), having d values of 55.5, 58.6, and 59.5 \AA , respectively. (b) Same as Fig. 8a, except the phase of the eighth-order lamellar Bragg reflection is + instead of -.



phase assignments result in a family of transforms that give an appearance of simplicity and uniqueness (Torbet and Wilkins 1976). Figure 8a contains the continuous Fourier transforms, reconstructed by use of the communication theorem (Shannon 1949), for DPPC bilayers in the L_{β} phase and which systematically expand outward in reciprocal space with increasing levels of hydration. This implies that with increasing hydration there is a decrease in the thickness of the bilayer (the motif) as a result of increases to the tilt angle θ (Tardieu et al. 1973; Katsaras et al. 1992b). Attempting to change the phase angle ϕ_h

Fig. 9. (a) 1D electron density distribution of 59.5 Å DPPC bilayers reconstructed from the structure factors obtained in Fig. 8a, and a 1D electron density distribution of 55.5 Å DPPC bilayers (b), reconstructed using an eighth-order Bragg reflection of + instead of - as predicted in Fig. 8a. One would expect a relatively uniform electron density corresponding to the methylene portion of the hydrocarbon chains. This is obviously not the case with the profile in Fig. 9b.



of a single reflection (e.g., eighth order + instead of -) results in a complicated family of transforms that do not exhibit any systematic changes with hydration (Fig. 8b). Finally, Fig. 9a shows the electron density distribution reconstructed from data in Fig. 8a, while Fig. 9b was reconstructed from data presented in Fig. 8b.

Applications to biological or biologically relevant systems

Model membrane systems are highly simplified compared with biological material. However, the techniques that we have described above have been used, sometimes successfully, to study biologically intact membrane multibilayer systems. One such system has been the structural determination of nerve myelin, whose 1D electron density profile (e.g., Worthington and McIntosh 1973) was determined using the swelling concept discussed in the solving of the phase problem and reconstruction of the electron density profiles section. Nerve myelin membrane can be swollen by use of different concentrations of glycerol or sucrose solutions, and since the structure is centrosymmetric, the phase choice for any one reflection is reduced to $\pm\sqrt{I_h}$, as was the case in the lipid bilayers previously discussed. Using the same swelling method, 1D electron density profiles of bleached and unbleached rod photoreceptor membranes (e.g., Corless 1972) and functional sarcoplasmic reticulum membranes (Herbette et al. 1977) were obtained.

The above examples are of biological systems that, as a result of their inherent structure, were suitable material to be studied directly using X-ray diffraction. However, if the investigation of a molecule is too difficult to be made in situ, then one can create a reconstituted system that is much simpler, in hopes of extracting some useful information. One such example was one in which the helical pitch of the gramicidin channel was determined in oriented gel and liquid - crystalline phase lipid bilayers (Katsaras et al. 1992a). The diffraction data was also consistent with the notion that the gramicidin molecule was a five-turn helix. For further examples of naturally occurring membrane multibilayers and model membranes as studied by X-ray diffraction, we refer the reader to the excellent article by Blaurock (1982).

Acknowledgements

The author thanks V.A. Raghunathan, the Centre de Recherche Paul Pascal (Bordeaux, France), and the Natural Sciences and Engineering Research Council of Canada.

References

- Amemiya, Y., and Wakabayashi, K. 1991. Imaging plate and its application to X-ray diffraction of muscle. *Adv. Biophys.* **27**: 115-128.
- Amemiya, Y., Satow, Y., Matsushita, T., Chikawa, J., Wakabayashi, K., and Miyahara, J. 1988. A storage phosphor detector (imaging plate) and its application to diffraction studies using synchrotron radiation. *Topics Curr. Chem.* **147**: 121-144.
- Bentz, J., Alford, D., and Ellens, H. 1992. Liposomes, membrane fusion, and cytoplasmic delivery. *In* The structure of biological membranes. Edited by P. Yeagle. CRC Press, Boca Raton, Fla. pp. 915-947.
- Blaurock, A.E. 1982. Evidence of bilayer structure and of membrane interactions from X-ray diffraction analysis. *Biochim. Biophys. Acta*, **650**: 167-207.
- Caciuffo, R., Melone, S., Rustichelli, F., and Boeuf, A. 1987. Monochromators for X-ray synchrotron radiation. *Phys. Rep.* **152**: 1-71.
- Chen, S.C., Sturtevant, J.M., and Gaffney, B.J. 1980. Scanning calorimetric evidence for a third phase transition in phosphatidylcholine bilayers. *Proc. Natl. Acad. Sci. U.S.A.* **77**: 5060-5063.
- Corless, J.M. 1972. Lamellar structure of bleached and unbleached rod photoreceptor membranes. *Nature (London)*, **237**: 229-231.

- Cullity, B.D. 1978. Elements of X-ray diffraction. 2nd ed. Addison-Wesley Publishing Company, Inc., Reading, Mass.
- Franks, N.P., and Lieb, W.R. 1981. X-ray and neutron diffraction studies of lipid bilayers. In *Liposomes: from physical structure to therapeutic applications*. Edited by C.G. Knight. Elsevier/North-Holland Biomedical Press, Amsterdam. pp. 242–272.
- Füldner, H.H. 1981. Characterization of a third phase transition in multilamellar dipalmitoyllecithin liposomes. *Biochemistry*, **20**: 5707–5710.
- Gruner, S.M. 1992. Nonlamellar lipid phases. In *The structure of biological membranes*. Edited by P. Yeagle. CRC Press, Boca Raton, Fla. pp. 211–250.
- Hentschel, M., Hosemann, R., and Helfrich, W. 1980. Direct X-ray study of the molecular tilt in dipalmitoyl lecithin bilayers. *Z. Naturforsch. A*, **35**: 643–644.
- Hentschel, M.P., and Rustichelli, F. 1991. Structure of the ripple phase P_{β} in hydrated phosphatidylcholine multimembranes. *Phys. Rev. Lett.* **66**: 903–906.
- Herbette, L., Marquardt, J., Scarpa, A., and Blasie, J.K. 1977. A direct analysis of lamellar X-ray diffraction from hydrated oriented multilayers of fully functional sarcoplasmic reticulum. *Biophys. J.* **20**: 245–272.
- Katsaras, J. 1995. Structure of the subgel (L_{α}) and gel (L_{β}) phases in oriented dipalmitoyl phosphatidylcholine multibilayers. *J. Phys. Chem.* **99**: 4141–4147.
- Katsaras, J., Stinson, R.H., Davis, J.H., and Kendall, E.J. 1991. Location of two antioxidants in oriented model membranes: small-angle X-ray diffraction study. *Biophys. J.* **59**: 645–653.
- Katsaras, J., Prosser, R.S., Stinson, R.H., and Davis, J.H. 1992a. The constant helical pitch of the gramicidin channel in phospholipid bilayers. *Biophys. J.* **61**: 827–830.
- Katsaras, J., Yang, D.S.-C., and Eppard, R.M. 1992b. Fatty-acid chain tilt angles and directions in dipalmitoyl phosphatidylcholine bilayers. *Biophys. J.* **63**: 1170–1175.
- Katsaras, J., Jeffrey, K.R., Yang, D.S.-C., and Eppard, R.M. 1993. Direct evidence for the partial dehydration of phosphatidylethanolamine bilayers on approaching the hexagonal phase. *Biochemistry*, **32**: 10 700–10 707.
- Katsaras, J., Raghunathan, V.A., Dufourc, E.J., and Dufourcq, J. 1995. Evidence for a 2D molecular lattice in subgel phase DPPC bilayers. *Biochemistry*, **34**: 4684–4688.
- Leadbetter, A.J., Gaugan, J.P., Kelly, B., Gray, G.W., and Goodby, J. 1979. Characterisation and structure of some new smectic F phases. *J. Phys.* **40**: C3-178 – C3-184.
- Levine, Y.K. 1973. X-ray diffraction studies of membranes. *Prog. Surf. Sci.* **3**: 279–352.
- McIntosh, T.J., and Simon, S.A. 1993. Contributions of hydration and steric (entropic) pressures to the interactions between phosphatidylcholine bilayers: experiments with the subgel phase. *Biochemistry*, **32**: 8374–8384.
- Mitsui, T. 1978. X-ray diffraction studies of membranes. *Adv. Biophys.* **10**: 97–135.
- Phillips, W.C. 1985. X-ray sources. *Methods Enzymol.* **114**: 300–316.
- Phillips, W.C., and Rayment, I. 1985. Systematic method for aligning double-focusing mirrors. *Methods Enzymol.* **114**: 316–329.
- Ruocco, M.J., and Shipley, G.G. 1982. Characterization of the sub-transition of hydrated dipalmitoylphosphatidylcholine bilayers. *Biochim. Biophys. Acta*, **684**: 59–66.
- Sayre, D. 1952. Some implications of a theorem due to Shannon. *Acta Crystallogr.* **5**: 843.
- Shannon, C.E. 1949. Communication in the presence of noise. *Proc. Inst. Radio Eng. N.Y.* **37**: 10–21.
- Singer, S.J., and Nicolson, G.L. 1972. The fluid mosaic model of the structure of cell membranes. *Science (Washington, D.C.)*, **175**: 720–731.
- Smith, G.S., Sirota, E.B., Safinya, C.R., and Clark, N.A. 1988. Structure of the L_{β} phases in a hydrated phosphatidylcholine multimembrane. *Phys. Rev. Lett.* **60**: 813–816.
- Smith, G.S., Sirota, E.B., Safinya, C.R., Plano, R.J., and Clark, N.A. 1990. X-ray structural studies of freely suspended ordered hydrated DMPC multimembrane films. *J. Chem. Phys.* **92**: 4519–4529.
- Stümpel, J., Eibl, H., and Nicksch, A. 1983. X-ray analysis and calorimetry on phosphatidylcholine model membranes: the influence of length and position of acyl chains upon structure and phase behaviour. *Biochim. Biophys. Acta*, **727**: 246–254.
- Tardieu, A., Luzzati, V., and Reman, F.C. 1973. Structure and polymorphism of the hydrocarbon chains of lipids: a study of lecithin-water phases. *J. Mol. Biol.* **75**: 711–733.
- Torbet, J., and Wilkins, M.H.F. 1976. X-ray diffraction studies of lecithin bilayers. *J. Theor. Biol.* **62**: 447–458.
- Tristram-Nagle, S., Zhang, R., Suter, R.M., Worthington, C.R., Sun, W.-J., and Nagle, J.F. 1993. Measurement of chain tilt angle in fully hydrated bilayers of gel phase lecithins. *Biophys. J.* **64**: 1097–1109.
- Tristram-Nagle, S., Suter, R.M., Sun, W.-J., and Nagle, J.F. 1994. Kinetics of subgel formation in DPPC: X-ray diffraction proves nucleation-growth hypothesis. *Biochim. Biophys. Acta*, **1191**: 14–20.
- Wakabayashi, K., and Amemiya, Y. 1991. Progress in X-ray synchrotron diffraction studies of muscle contraction. In *Handbook of synchrotron radiation*. Vol. 4. Edited by S. Ebashi, M. Koch, and E. Rubenstein. Elsevier Science Publishers, Amsterdam. pp. 597–678.
- Weiner, M.C., and White, S.H. 1992. Structure of a fluid dioleoylphosphatidylcholine bilayer determined by joint refinement of X-ray and neutron diffraction data. III. Complete structure. *Biophys. J.* **61**: 434–447.
- Wilkins, S.W., and Stevenson, A.W. 1988. A class of condensing-collimating channel-cut monochromators for SAXS, XRPD, and other applications. *Nucl. Instrum. Methods*, **A269**: 321–328.
- Worthington, C.R., and McIntosh, T.J. 1973. Direct determination of the electron density profile of nerve myelin. *Nature New Biol.* **245**: 97–99.

Notes about the author

Dr. John Katsaras, the author of this review, is a recipient of a postdoctoral fellowship from the Natural Sciences and Engineering Research Council of Canada (NSERC). Dr. Katsaras was born in Rhodes, Greece, and was raised in Montreal, Que., Canada. He did his undergraduate training at Concordia University in Montreal and then went on to do his graduate work on X-ray diffraction of model membrane systems under the supervision of Dr. Robert H. Stinson at the University of Guelph, Ont. After receiving his Ph.D., he was awarded a

Notes sur l'auteur

Dr. John Katsaras, l'auteur de cette revue, a reçu une bourse postdoctorale du Conseil de recherches en sciences naturelles et en génie du Canada (CRSNG). Dr. Katsaras est né à Rhodes en Grèce et a grandi à Montréal, Québec, Canada. Il a fait un baccalauréat à l'Université Concordia de Montréal. Puis, il a obtenu un Ph.D. après avoir complété un projet de recherche portant sur la diffraction des rayons X de modèles de membranes sous la direction du Dr. Robert H. Stinson à l'Université de Guelph en Ontario. Par la suite, il a obtenu une bourse

NSERC postdoctoral fellowship to work in the laboratory of Dr. Richard M. Eband at the McMaster University Health Sciences Centre, Hamilton, Ont., on fusogenic peptides, and in the laboratory of Dr. J. Dufourcq at the Centre de recherche Paul Pascal-CNRS, Bordeaux, France, on lamellar phases of DPPC. In 1994, after completing his postdoctoral work, Dr. Katsaras went to Atomic Energy of Canada Limited, Chalk River, Ont., where he presently holds a Research Associate position in the Department of Neutron and Condensed Matter Science.

postdoctorale du CRSNG pour étudier les peptides de fusionnement dans le laboratoire du Dr. Richard M. Eband au Centre des sciences de la santé de l'Université McMaster à Hamilton en Ontario et les phases lamellaires de la 1,2-dipalmityl-*sn*-glycéro-3-phosphatidylcholine (DPPC) dans le laboratoire du Dr. J. Dufourcq au Centre de recherche Paul Pascal - CNRS de Bordeaux, France. En 1994, après son stage postdoctoral, Dr. Katsaras a été employé par Énergie atomique du Canada limitée à Chalk River, Ontario. Il est présentement associé de recherche au Département des sciences du neutron et de la matière dense.